Electrochimica Acta 168 (2015) 82–88

Contents lists available at ScienceDirect

Electrochimica Acta

journal homepage: www.elsevier.com/locate/electacta

Anthracene mediated electrochemical synthesis of metallic cobalt nanoparticles in solution

Vitaliy V. Yanilkin [a,*], Gulnaz R. Nasretdinova [a], Yuri N. Osin [b], Vadim V. Salnikov [b]

[a] A.E Arbuzov Institute of Organic and Physical Chemistry, Kazan Scientific Center, Russian Academy of Sciences, Arbuzov St. 8, 420088 Kazan, Russia
[b] Kazan Federal University, Interdisciplinary Center of Analytical Microscopy, Kremlevskaya St. 18, 420018 Kazan, Russia

ARTICLE INFO

Article history:
Received 9 December 2014
Received in revised form 30 March 2015
Accepted 30 March 2015
Available online 2 April 2015

Keywords:
Electrochemical synthesis
Co^0 nanoparticle
Mediator
Anthracene

ABSTRACT

The metallic cobalt nanoparticles in the bulk solution were obtained by antracene mediated reduction of $[CoCl_4]^{2-}$ in the potentiostatic electrolysis in an undivided cell at the potential of the anthracene reduction to radical anion at room temperature in DMF/0.1 M Bu_4NCl media. $[CoCl_4]^{2-}$ ions are generated by the sacrificial cobalt anode dissolution during the electrolysis. The metal particles are oxidized upon contact with the air to form the oxidized cobalt nanoparticles with a low dispersity (20–30 nm).

1. Introduction

In recent years, the metal nanoparticles are of great scientific interest due to their unique physical and chemical properties different from those of bulk metals, and a wide variety of potential applications in the field of catalysis, biomedicine, optics, electronics and other [1–7]. Methods of preparation of metal nanoparticles are quite diverse. They are conventionally divided into physical, chemical and sometimes into biochemical ones. The electrochemical methods of obtaining of metal nanoparticles in solution have found only limited application [6–14], although the electrochemical reduction of the metal ions and complexes is the classical method of producing metals, metal plating, metal black on the electrode surface on an industrial scale [15]. This is primarily because the direct reduction of metal ions results in metal deposition on the electrode surface. For example, when using this method of producing silver nanoparticles in solution, up to 80 percent of the metal is deposited on the electrode surface [11]. The problem of deposition is partially solved by a combination of the metals accumulation process during a short current impulse followed by the metal transfer from the surface into the solution by means of sonification of the working electrode (pulse sonoelectrochemistry) [12–14].

It seems that another more efficient approach to implementation of the electrochemical process for production of metal and metal-alloy nanoparticles in solution can be a transfer of electroreduction reaction of ions or their complexes from the electrode surface into the solution using mediators. In the process of chemical synthesis of a finely-dispersed metal using alkali metals to reduce metal salts in ethereal or hydrocarbon solvents according to Rieke process, organic electron carriers (naphthalene, biphenyl, anthracene, etc.) are widely used as mediators [16–19]. The idea of using organic electron carriers for generating highly reactive metal (0) in solution by mediated electrochemical reduction of metal ions and metal complexes have been used by us to create highly efficient electrocatalytic systems for reduction of various organic substrates [20]. Based on this idea [20] recently an efficient electrosynthesis of palladium and silver nanoparticles have been carried out by the mediated reduction of $[PdCl_4]^{2-}$ in 60% aqueous DMF [21,22] and DMSO [23], anode-generated silver ions Ag^+ in DMF [24] using methylviologen MV^{2+} and/or tetraviologen calix[4]resorcine MVCA-C_n^{8+} (n = 1,5,10) with n-alkyl substituents in the resorcinol cycles as a mediator at potential of redox couples $MV^{2+}/MV^{\bullet+}$, MVCA-C_n^{8+}/MVCA-$C_n^{4\bullet+}$. Tetraviologen calix[4]resorcines also stabilized nanoparticles both in the solution and/or on the electrode surface. In this article, the electrochemical synthesis of cobalt nanoparticles in DMF/0.1 M Bu_4NCl using anthracene as a mediator is reported. Nanoparticles of cobalt and its alloys are of interest as catalysts [16,18] and magnetic materials [19,25]. Co^{2+} ions are reduced harder than the above-mentioned ions, so a reducing agent more effective than methylviologen radical cation is required to reduce them. Therefore, the choice of a medium and a mediator is made on the basis of earlier [20] findings of the reduction of cobalt ions by anthracene radical anion.

* Corresponding author.
E-mail address: yanilkin@iopc.ru (V.V. Yanilkin).

http://dx.doi.org/10.1016/j.electacta.2015.03.214
0013-4686/

2. Experimental section

The investigation was carried out using the methods of cyclic voltammetry (CV), electrolysis, dynamic light scattering (DLS) and scanning electron microscopy (SEM).

The CV recordings were done with a P-30S potentiostat (without IR-compensation) in argon atmosphere. The working electrode was a glassy carbon disk electrode (∂ = 2 mm) brazed in glass. The electrode was cleaned by mechanical polishing with diamond paste before each measurement. Platinum wire was a counter electrode. The potentials were measured relative to the aqueous saturated calomel electrode (SCE), E_0' (Fc/Fc^+) = +0.41 V. Aqueous SCE was connected by a bridge filled with supporting solution. The temperature was 295 K. The diffusion nature of the peak currents i_p was proven using the theoretical shape of the voltammogram and the linear dependence $i_p - \nu^{1/2}$ by varying the potential scan rate ν from 10 to 200 mV/s, and the adsorption nature was substantiated by the presence of an adsorption maximum.

Anthracene, $Co(BF_4)_2 \cdot 6H_2O$, the supporting electrolytes Bu_4NBF_4 (Aldrich), Bu_4NCl (Fluka) and the solvent N,N-dymethylformamide (DMF) (Alfa Aesar) were used as purchased without additional purification.

The microelectrolysis was carried out in a three electrode undivided glass cell in a potentiostatic mode in argon atmosphere at room temperature (T = 295 K) using a P-30S potentiostat. During the electrolysis, the solution (DMF, 0.1 M Bu_4NCl, 2 mM Anthracene, V = 20 ml) was stirred with a magnetic stirrer. Glassy carbon tissue was the cathode (S = 10 cm^2); a cobalt plate (S = 4.2 cm^2) was the anode; and SCE was the reference electrode. SCE was connected by a bridge filled with supporting solution.

When the electrolysis was over the solution was controlled by CV on the indicator glassy carbon disk electrode (∂ = 2 mm) directly in the electrolyzer, and then, the metal particles formed in the process of electrolysis were analyzed with DLS and SEM.

The DLS measurements were performed using Malvern Instrument Zetasizer Nano. The measured autocorrelation functions were analyzed with Malvern DTS software.

For carrying out the electron microscopic analysis the solution was applied to the surface of the titanium foil was previously cleared by sonification in acetone. Then the sample was exsiccated at low heat (not above 40 °C). The morphology of the SAMPLE surfaces was characterized in plan-view with SEM using a high-resolution microscope Merlin of Carl Zeiss combined with ASB (Angle Selective Backscattering) and SE InLens (Secondary Electrons Energy selective Backscattering) detectors, which was also equipped for energy-dispersive X-ray spectroscopy (EDX) analysis with AZTEC X-MAX energy-dispersion spectrometer from Oxford Instruments.

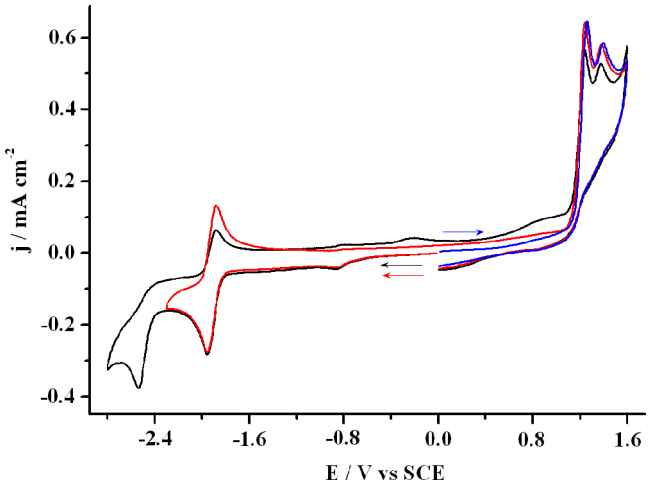

Fig. 1. CV curves of anthracene (1 mM) in DMF/0.1 M Bu_4NBF_4 media using a glassy carbon electrode. ν = 100 mV/s.

3. Results and discussions

3.1. DMF/0.1 M Bu_4NBF_4 media

The cyclic voltammogram (CV) of anthracene recorded using a glassy carbon electrode exhibits two diffusion one-electron reduction peaks in the cathodic potential region, the first one is reversible while the second is not (Fig. 1,Table 1). According to the literature [20,26], a stable radical anion forms at the first peak potential, while a dianion forms at the potentials of the second peak which undergoes rapid irreversible chemical transformations. Two poorly separated irreversible oxidation peaks are recorded on the anode region. The first peak ($E_{p,ox}$ = 1.27 V) is dominant and the second is faint.

Co^{2+} ions are reduced significantly easier than anthracene, the reduction peak is sharp, irreversible and diffusion-controlled (Fig. 2, Table 1). Two re-oxidation peaks are observed at potentials near zero and 1.48 V on the reverse part of the CV curve, the first peak is the adsorption. With the increase of Co^{2+} ions concentration the reduction peak and the first reoxidation peak increase proportionally, while the second reoxidation peak somewhat decreases. The rise of the oxidation current of bulk metallic cobalt to form Co^{2+} starts from almost zero volts in this medium (Fig. 3). Evidently, the recorded reduction peak of Co^{2+} corresponds to its two-electron reduction to $(Co^0)_n$, which is deposited on the electrode and is oxidized at the first reoxidation peak potential. The high steepness of the Co^{2+} reduction peak (Table 1) is due to the easier Co^{2+} ions reduction on the as-deposited cobalt particles,

Table 1
The characteristics of the reduction and reoxidation peaks of anthracene (1.0 mM), Co(II) (2.0 mM), obtained by CV using a glassy carbon electrode in DMF/0.1 M $Bu_4N^+X^-$ media.

Substrate	X^-	$E_{p,red}{}^1$, V	$E_{p,red}{}^1 - E_{p/2,red}{}^1$, mV	$j_{p,red}{}^1$, mA cm^{-2}	$E_{p,reox}{}^1$, V	$E_{p,red}{}^2$, V	$E_{p,reox}{}^2$, V	$E_{p,reox}{}^3$, V
anthracene	BF_4	−1.95	62	0.26	−1.89	−2.53	–	–
+ Co^{2+}		−1.15	26	0.74	0.01	–	1.48	–
anthracene + Co^{2+}		−1.21	50	0.70	−1.87	−1.97	−0.05	–
anthracene	Cl	−1.92	65	0.26	−1.85	−2.51	–	–
Co^{2+}		−2.22	137	0.55	−0.44	–	0.72	–
anthracene + Co^{2+}		−1.97	98	0.76	−0.54	–	−0.02	0.68

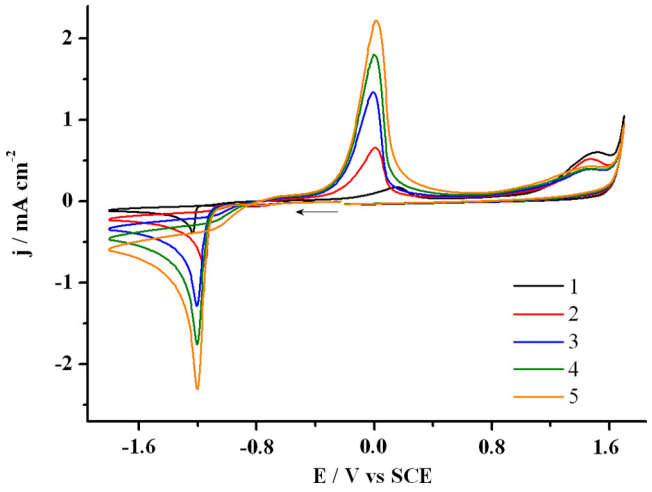

Fig. 2. CV curves of Co^{2+} in DMF/0.1 M Bu_4NBF_4 media using a glassy carbon electrode at the concentration, mM: (1) 1, (2) 2, (3) 3, (4) 4, (5) 5. ν = 100 mV/s.

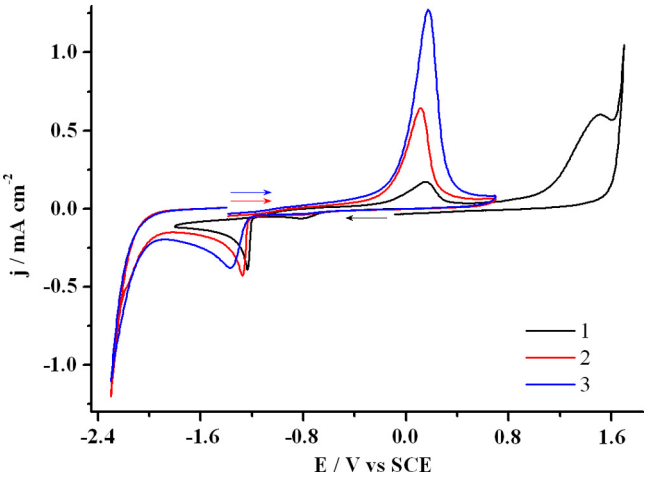

Fig. 4. CV curves of Co^{2+} (1 mM) in DMF/0.1 M Bu_4NBF_4 media using a glassy carbon electrode: (1) the initial solution; after the applying the potential E = −1.4 V for (2) 1 min, (3) 3 min. ν = 100 mV/s.

that is consistent with the decrease in the reduction current at less cathodic potentials on the reverse CV curve (unusual hysteresis curve for the CV). The same factor determines some dependence of the peak potential on Co^{2+} ions concentration (Fig. 2) and the facility of the reduction of the supporting solution in the presence of cobalt ions. The rise of the reduction current of the supporting solution starts at −2.8 V on the glassy carbon electrode and at −2.3 V on the glassy carbon electrode with deposited cobalt. As for the second reoxidation peak, the nature of the processes is not sufficiently clear. Metal deposition and following its dissolution results, probably, in the glassy carbon electrode surface activation and easier oxidation of the supporting electrolyte on such electrode that is formally recorded as the second reoxidation peak on the CV curve.

The number of $(Co^0)_n$ particles on the electrode surface is increased after applying the fixed potential E = −1.4 V (i.e. the potential of Co^{2+} reduction) without stirring the solution that is evident from the increase in their re-oxidation peak (Fig. 4). Upon oxidation of these particles, Co^{2+} ions are formed again and are reduced a little harder than on the initial electrode (Fig. 4).

The CV curve of anthracene and Co^{2+} mixture is an additive curve of the individual components at all investigated ratios (from 1:1 to 1:5) (Fig. 5), which indicates the independence of their reduction under the CV curve recording conditions.

In presence of anthracene the direct Co^{2+} reduction on the electrode at E = −1.4 V during different periods of time without stirring the solution results in the accumulation of $(Co^0)_n$ particles on the electrode surface. Anthracene is not accumulated as the permanent height of its first oxidation peak indicates (Fig. 6). The oxidation of the deposited metal particles leads again to the formation of Co^{2+} that follows from the increase of their reduction peak on the reverse part of the CV curve (Fig. 6). Consequently, electrochemical behavior of Co^{2+} ions in presence of anthracene is the same as in its absence, and the deposited metal particles are not bound with anthracene.

The presence of anthracene in the solution influences the properties of the produced metal particles at the potential of the radical anions generation only. After applying the potential of anthracene first reduction peak (E = −2.1 V), the reoxidation peaks of the anthracene radical anions and the oxidation peaks of anthracene are recorded with initial intensity on the CV while the reoxidation peak of the cobalt particles $(Co^0)_n$ is absent (Fig. 7). The Co^{2+} reduction peak decreases with the increase of the incubation

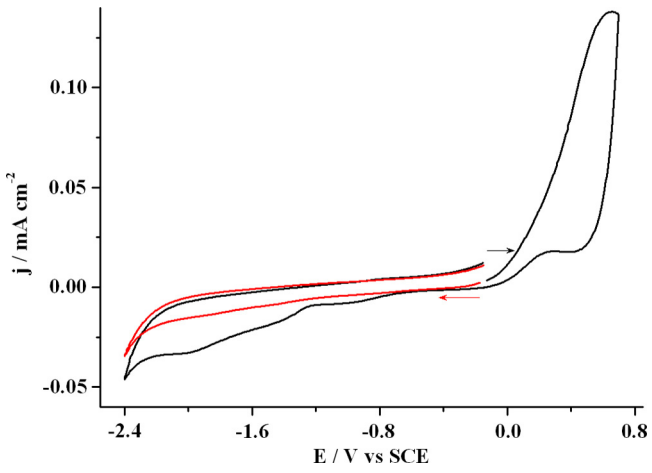

Fig. 3. CV curves at the Co electrode (S = 4.2 cm^2) in DMF/0.1 M Bu_4NBF_4 media, ν = 100 mV/s.

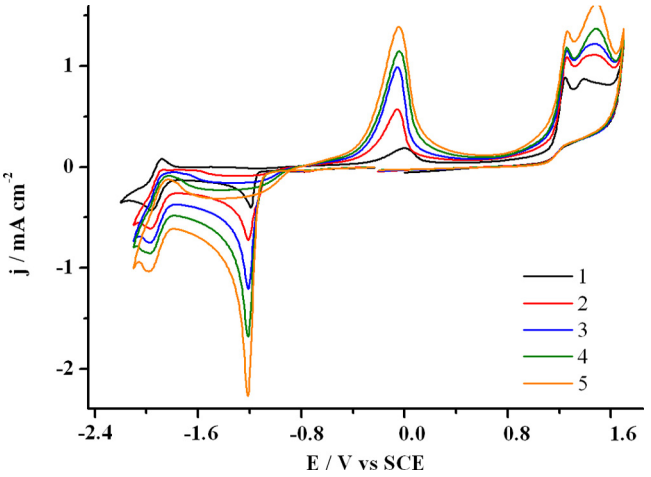

Fig. 5. CV curves of the system anthracene (1 mM) – Co^{2+} in DMF/0.1 M Bu_4NBF_4 media using a glassy carbon electrode at the concentration of Co^{2+}, mM: (1) 1, (2) 2, (3) 3, (4) 4, (5) 5. ν = 100 mV/s.

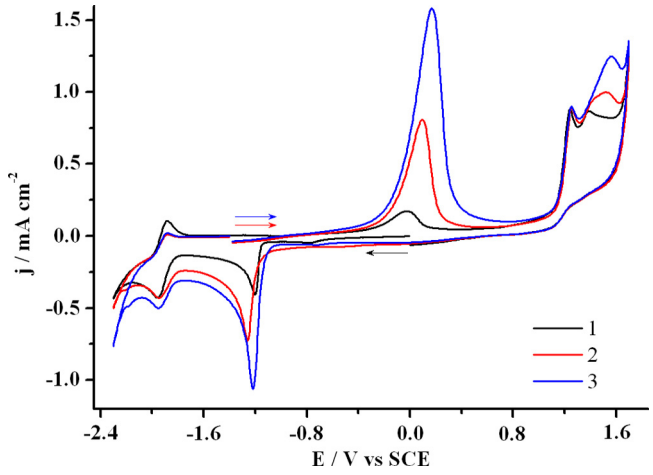

Fig. 6. CV curves of the system anthracene (1 mM) – Co^{2+} (1 mM) in DMF/0.1 M Bu_4NBF_4 media using the glassy carbon electrode: (1) the initial solution; after the applying potential E = −1.4 V for (2) 1 min, (3) 3 min. ν = 100 mV/s.

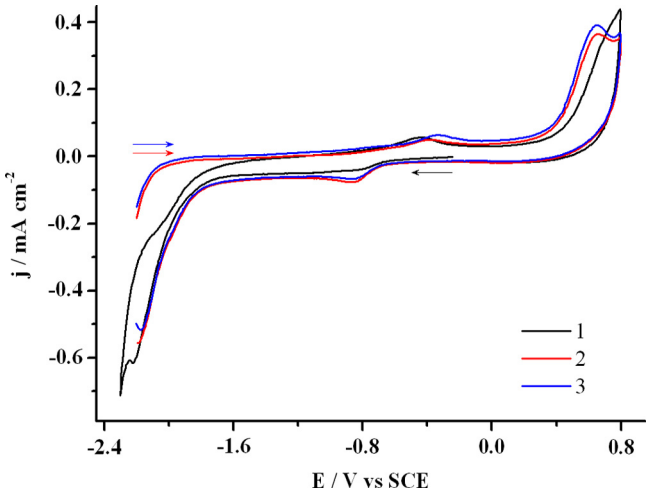

Fig. 8. CV curves of $[CoCl_4]^{2-}$ (2 mM) in DMF/0.1 M Bu_4NCl media using a glassy carbon electrode: (1) the initial solution; after the applying potential En = −2.2 V for (2) 1 min, (3) 3 min. ν = 100 mV/s.

time, i.e. during the electrolysis at this potential the near-electrode layer is depleted in Co^{2+} ions due to their reduction.

The results lead to the following conclusions:

(i) the electrochemically generated anthracene radical anions effectively reduce Co^{2+} ions at room temperature in DMF/0.1 M Bu_4BF_4 media;
(ii) the mediated electrochemical reduction of Co^{2+} ions at the potential of anthracene radical anions generation is not accompanied with deposition of the measurable amounts of metal on the electrode surface.

3.2. DMF/0.1 M Bu_4NCl media

The replacement of BF_4^- anion of the supporting electrolyte with Cl^- does not affect the cathodic region of the anthracene CV curve, but results in the following: (i) the limitation of the anodic potential region to 0.8 V due to oxidation of chloride ions, therefore anthracene oxidation potential is not achieved; (ii) the Co^{2+} reduction peak shift to 1.07 V in the negative direction (Table 1) due to the formation of blue dianion complex $[CoCl_4]^{2-}$ [27]. In contrast to Co^{2+}, this dianion reduces harder than anthracene near the reduction potential of the supporting solution, so its peak is poorly expressed (Fig. 8). The reduction products are oxidized at −0.44 V and +0.72 V. Bulk metallic cobalt begins to oxidize at zero volts. Oxidation begins at −0.4 V on the activated surface that follows the reverse CV curve (Fig. 9). Consequently, the peak at −0.44 V relates to the metal particles oxidation. Interestingly, in this case, their number on the electrode surface is not increased with the increase in the reduction time (Fig. 8).

The first reduction peak of anthracene increases after adding $[CoCl_4]^{2-}$ to the anthracene solution (Fig. 10). And the reoxidation peak of the metal particles appears at the same potentials as in the absence of anthracene on the reverse part of the CV curve (Fig. 10). The effects on both peaks increase with the increase of $[CoCl_4]^{2-}$ concentration. The reduction peak of the complex dianion is absent on the CV at all the investigated ratios of anthracene and $[CoCl_4]^{2-}$ (from 1:1 to 1:5). Obviously, the effective mediated

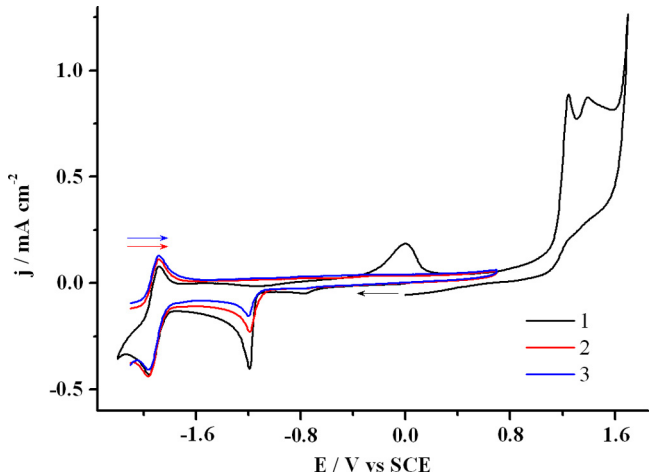

Fig. 7. CV curves of the system anthracene (1 mM) – Co^{2+} (1 mM) in DMF/0.1 M Bu_4NBF_4 media using a glassy carbon electrode: (1) the initial solution; after the applying potential E = −2.1 V for (2) 1 min, (3) 3 min. ν = 100 mV/s.

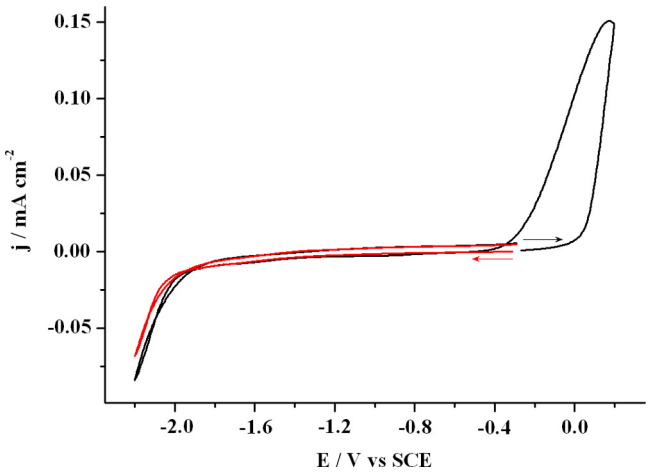

Fig. 9. CV curves at the Co electrode (S = 4.2 cm^2) in DMF/0.1 M Bu_4NCl media. ν = 100 mV/s.

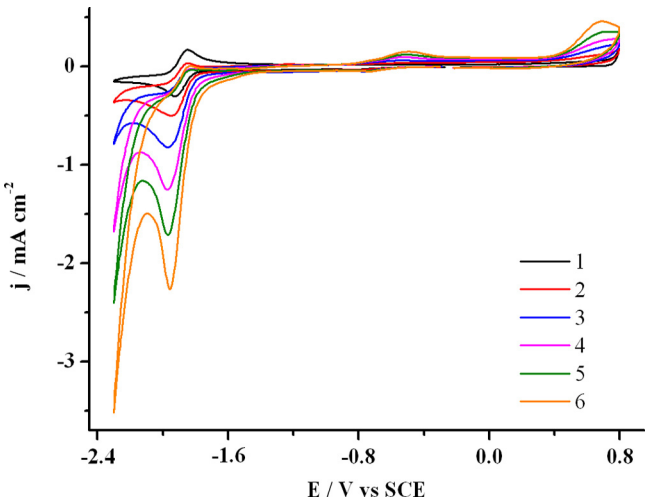

Fig. 10. CV curves of the system anthracene (1 mM) – $[CoCl_4]^{2-}$ in DMF/0.1 M Bu_4NCl media using the glassy carbon electrode at the concentration of Co^{2+}, mM: (1) 0, (2) 1, (3) 2, (4) 3, (5) 4, (6) 5. ν = 100 mV/s.

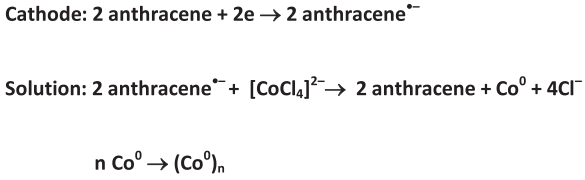

Scheme 1. Mediated reduction of $[CoCl_4]^{2-}$ using anthracene as mediator.

electrochemical reduction of $[CoCl_4]^{2-}$ occurs at the potential of anthracene radical anions generation at the diffusion rate of dianion complex to the electrode surface (Scheme 1).

The products of more prolonged reduction are metal particles of different size which are, therefore, oxidized at different potentials [28]. At least four poorly defined oxidation peaks are obtained on the CV curve. As far as the peak intensity does not change with the increase of the electrolysis time, it is possible to say that the mediated generated metal particles are not noticeably deposited on the electrode.

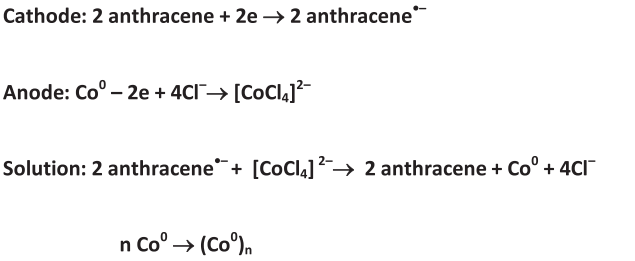

Scheme 2. The mediated electrosynthesis of metallic cobalt nanoparticles $(Co^0)_n$ using anthracene as a mediator and metallic cobalt as a supplier of Co^{2+}.

Thus, according to cyclic voltammetry, the effectively mediated Co^{2+} ions reduction is possible at the potentials of anthracene radical anion generation in the both investigated media. Co^{2+} ions can be added into the initial solution once or are generated by dissoluting the anode during the electrolysis. In the first case, the electrolysis should be carried out in the cathode compartment of a diaphragm cell, while in the second case, a simpler electrolysis in an undivided cell with a cobalt anode is to be used. The easier way was chosen. Cobalt anode is activated in presence of Cl^-, (Fig. 3). So Bu_4NCl was chosen as a supporting electrolyte to lower the oxidation potential.

3.3. Preparative electrolysis

The electrolysis of anthracene solution (2 mM) was carried out at the controlled potential of the anthracene first reduction peak (E = −2.3 V) in an undivided cell in DMF/0.1 M Bu_4NCl using a glassy carbon tissue as a cathode and a cobalt plate as an anode. The current remains almost constant (∼−25 mA) and $8.34 \cdot 10^{-5}$ F (i.e. 2F/mol anthracene) was ran throughout the electrolysis. During the electrolysis, the weight of the cobalt plate decreased by 2 mg, which corresponds to the theoretical value (2.4 mg) calculated by the Faraday's law for two-electron dissolution of cobalt to Co^{2+}. The pinkish color of the solution turned dark brown and the solution after the electrolysis remained fully homogeneous. The anthracene first reduction peak is of the same intensity after the electrolysis, as it was before the electrolysis on the CV (Fig. 11). The metal particles oxidation peak is recorded at $E_{p,ox}$ = −0.11 V in the anode region. The peak intensity is not increased after the electrode has stayed in the solution for 3 minutes without stirring and without an overlaying potential. To summarize, these data lead to the

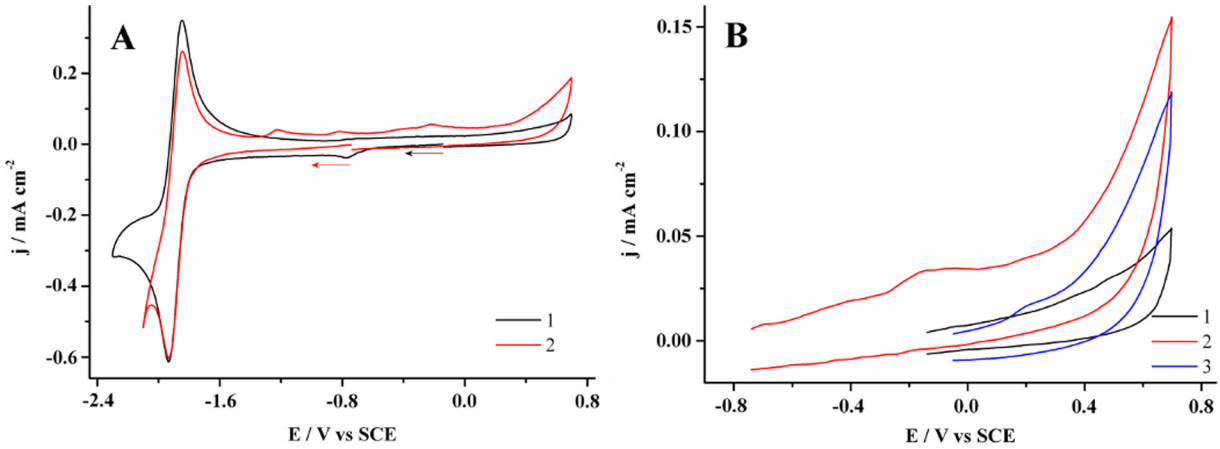

Fig. 11. CV curves of the system anthracene (2 mM) – Co^0 in DMF/0.1 M Bu_4NCl media using the glassy carbon electrode (1) before and (2) after the electrolysis at E = −2.3 V (Q = 2 F/mol anthracene), and (3) in an hour after the electrolysis with the potential scan in (A) negative and (B) positive directions. ν = 100 mV/s.

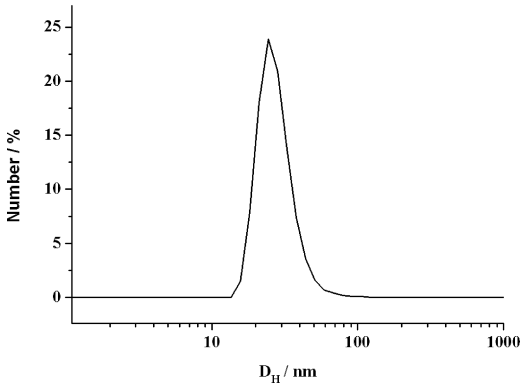

Fig. 12. Size distribution diagrams of ≪oxidized≫ Co nanoparticles obtained after the electrolysis.

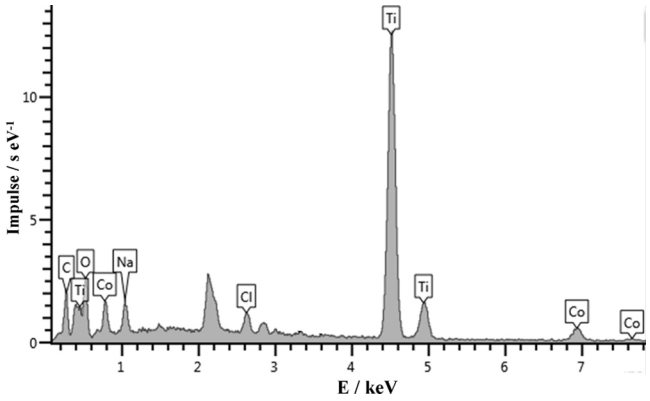

Fig. 14. The qualitative analysis of ≪oxidized≫ Co particles composition deposited onto a titanium foil using the solvent evaporation method.

following conclusions: (i) the metal cobalt is quantitively dissolved to produce Co^{2+} ions; (ii) $[CoCl_4]^{2-}$ is absent from the solution after the electrolysis; (iii) anthracene really functions only as a mediator and is absolutely not expended; (iv) an effective quantitative transfer of bulk metallic cobalt(0) to the metallic cobalt(0) nanoparticles in the solution occurs in the process of electrolysis, (Scheme 2); (v) cobalt nanoparticles are not adsorbed on the electrode surface.

Unlike Pd and Ag nanoparticles [21–24], the Co nanoparticles generated under these conditions are oxidized with oxygen; therefore the deep dark brown solution is quickly decolorized upon contact with the air and becomes dark green. This color is preserved for at least a week. The metal oxidation peak is also observed on the CV curve of the "oxidized" solution but it is much less intense and occurs at a more positive potential $E_{p,ox} = 0.21$ V. According to the dynamic light scattering (DLS) data, the average hydrodynamic diameter of the oxidized metal particles is 24 nm (PdI = 0.448 ± 0.027) (Fig. 12). Apparently, cobalt remains a metal only in the center of nanoparticles and exists in the form of oxides in the outward part.

According to the scanning electron microscopy (SEM), the solid phase obtained after deposition onto titanium foil by the solvent evaporation method also has particles in the same size range (generally 20–30 nm) (Fig. 13A). However, in this case, all other components (anthracene and Bu_4NCl) of the solution except metal are also deposited, therefore it is not possible to determine the nanoparticles nature. This is why the nanoparticles was separated by centrifugation (15 000 rpm) for 2 hours. The brown precipitate is deposited on the walls of the test tube; it was separated from the solution; was washed with acetone and was dispersed in double-distilled water by sonification. The resulting solution was again examined using the same SEM procedure (Fig. 13B). The qualitative elemental analysis shows the presence in the sample of mainly cobalt, oxygen, carbon and chlorine (Fig. 14), i.e. cobalt oxide and some Bu_4NCl. In this case, smaller sized (5–10 nm) nanoparticles are also found in a much smaller quantity. The considerable amount of the oxidized metal is in the form of larger particles.

4. Conclusions

Previously [21–24], a high efficiency of the new method developed by us for the mediated electrosynthesis of a fine metal in a liquid phase using the mediated reduction of their ions or complexes has been shown exemplified by the palladium and silver nanoparticles. In this study, a high efficiency of the method has been demonstrated for the synthesis of cobalt nanoparticles by using anthracene as a mediator in the electrolysis at the potential of anthracene reduction to the radical anion in aprotic DMF and generating $[CoCl_4]^{2-}$ ions by dissolving the bulk cobalt anode during the electrolysis. The cobalt nanoparticles are oxidized by atmospheric oxygen that indicates the accessibility of the surface and high reactivity.

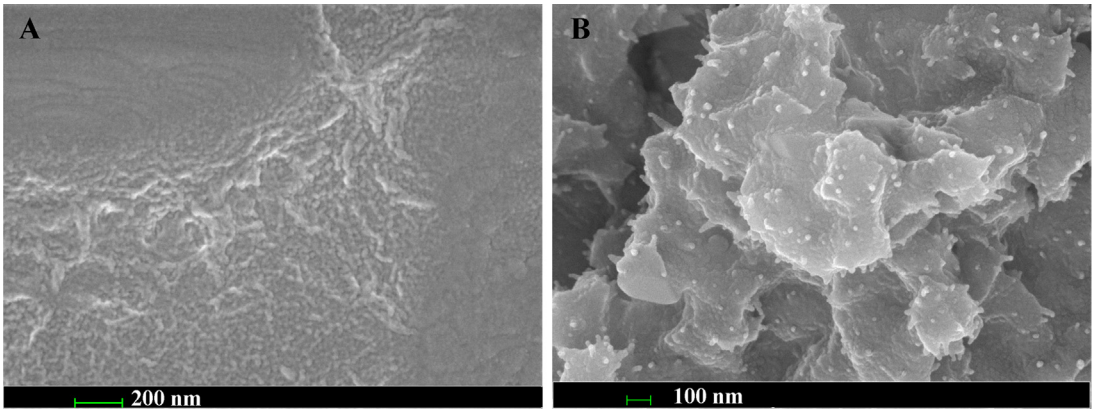

Fig. 13. SEM images of Co^0 nanoparticles deposited onto a titanium foil using the solvent evaporation method (A) after electrolysis and (B) after the following separation and dispergation in water by sonification.

Acknowledgment

The authors thank the RSF for a financial support (grant no. 14-23-00016).

References

[1] A.D. Pomogaylo, A.S. Rosenberg, I.E. Uflyand, Nanoparticles of metals in polymers, "Khimia", Moscow, 2002.
[2] V.I. Roldughin, Quantum-size colloid metal systems, Russ. Chem. Rev. 69 (2000) 821–843.
[3] M.C. Daniel, D. Astruc, Gold nanoparticles: assembly, supramolecular chemistry, quantum-size-related properties, and applications toward biology, catalysis, and nanotechnology, Chem. Rev. 104 (2004) 293–346.
[4] I.P. Suzdalev, Nanotechnology. Physicochemistry of nanoclusters, nanostructures and nanomaterials, "KomKniga", Moscow, 2006.
[5] V.V. Volkov, T.A. Kravchenko, V.I. Roldughin, Metal nanoparticles in catalytic polymer membranes and ion-exchange systems for advanced purification of water from molecular oxygen, Russ. Chem. Rev. 82 (2013) 465–482.
[6] L.A. Dykman, V.A. Bogatyrev, Gold nanoparticles: preparation, functionalisation and applications in biochemistry and immunochemistry, Russ. Chem. Rev. 76 (2007) 181–194.
[7] B.I. Kharisov, O.V. Kharissova, U. Ortiz-Mendez, Handbook of less-common nanostructures, CRC Press, 2012.
[8] M.T. Reetz, W. Helbig, Size-selective synthesis of nanostructured transition metal clusters, J. Am. Chem. Soc. 116 (1994) 7401–7402.
[9] J.A. Becker, R. Schäfer, R. Festag, W. Ruland, J.H. Wendorff, J. Pebler, S.A. Quaiser, W. Helbig, M.T. Reetz, Electrochemical growth of superparamagnetic cobalt clusters, J. Chem. Phys. 103 (1995) 2520–2527.
[10] L. Rodrigues-Sanchez, M.L. Blanko, M.A. Lopez-Quintela, Electrochemical synthesis of silver nanoparticles, J. Phys. Chem. 104 (2000) 9683–9688.
[11] I.E. Gracheva, G.N. Kreizberg, I.V. Golikov, Electrochemical synthesis of silver nanoparticles, FEN-Nauka 1 (2011) 7–9.
[12] V. Saez, T.J. Mason, Sonoelectrochemical synthesis of nanoparticles, Molecules 14 (2009) 4284–4299.
[13] J. Zhu, S. Liu, O. Palchik, Yu. Koltypin, A. Gedanken, Shape-controlled synthesis of silver nanoparticles by pulse sonoelectrochemical methods, Langmuir 16 (2000) 6396–6399.
[14] J. Reisse, T. Caulier, C. Deckerkheer, O. Fabre, J. Vandercammen, J.L. Delplancke, R. Winand, Quantitative sonochemistry, Ultrasonics Sonochemistry 3 (1996) 147–151.
[15] A.M. Sukhotin, Reference book of electrochemistry, "Khimia", Leningrad, 1981.
[16] R.D. Rieke, Preparation of highly reactive metal powders and their use in organic and organometallic compounds, Acc. Chem. Res. 10 (1977) 301–306.
[17] R.D. Rieke, Preparation of highly reactive powders/surfaces and their use in the preparation of organometallic compounds, Crit. Rev. Surf. Chem. 1 (1991) 131–166.
[18] A. Fürstner, Active Metals: Preparation, Characterization, Applications, John Wiley & Sons, 2008.
[19] D. Leslie-Pelecky, M. Bonder, T. Martin, E.M. Kirkpatrick, X.Q. Zhang, S.-H. Kim, R.D. Reike, Chemical synthesis of nanostructured cobalt at elevated temperatures, IEEE Trans. Magn. 34 (1998) 1018–1020.
[20] V.V. Yanilkin, N.I. Maksimyuk, E.I. Strunskaya, The double mediator system: organic electron carrier – metal ions in the electrochemical reduction of bromo- and chlororganic compounds, Russ. J. Electrochem. 32 (1996) 130–137.
[21] V.V. Yanilkin, G.R. Nasybullina, A. Yu. Ziganshina, I.R. Nizamiev, M.K. Kadirov, D.E. Korshin, A.I. Konovalov, Tetraviologen calix[4]resorcine as a mediator of the electrochemical reduction of $[PdCl_4]^{2-}$ for the production of Pd^0 nanoparticles, Mendeleev Commun. 24 (2014) 108–110.
[22] V.V. Yanilkin, G.R. Nasybullina, E.D. Sultanova, A. Yu. Ziganshina, A.I. Konovalov, Methyl viologen and tetraviologen calix[4]resorcinol as mediators of the electrochemical reduction of $[PdCl_4]^{2-}$ with formation of finely dispersed Pd^0, Russ. Chem. Bull. 63 (2014) 1409–1415.
[23] V.V. Yanilkin, N.V. Nastapova, G.R. Nasretdinova, R.K. Mukhitova, I.R. Ziganshina, M.K. Kadirov, Electrochemical synthesis of Pd^0 nanoparticles in solution, Russ. J. Electrochem. (2015) (in press).
[24] G.R. Nasretdinova, R.R. Fazleeva, R.K. Mukhitova, I.R. Nizameev, M.K. Kadirov, A. Yu Ziganshina, V.V. Yanilkin, Electrochemical synthesis of silver nanoparticles in solution, Electrochem. Comm. 50 (2015) 69–72.
[25] G. Yurkov, D.A. Baranov, I.P. Dotsenko, S.P. Gubin, New magnetic materials based on cobalt and iron-containing nanoparticles, Composites Part B 37 (2006) 413–417.
[26] C.K. Mann, K.K. Barnes, Electrochemical reactions in nonaqueous systems, Marcel Deccer, Inc., New York, 1970.
[27] M.H. Freemantle, Chemistry in action, Macmillan Education, London, 1987.
[28] W.J. Plieth, Electrochemical properties of small clusters of metal atoms and their role in surface enhanced Raman scattering, J. Phys. Chem. 86 (1982) 3166–3170.